МАТЕМАТИКА И МАТЕМАТИЧЕСКО ОБРАЗОВАНИЕ, 2009
MATHEMATICS AND EDUCATION IN MATHEMATICS, 2009
Proceedings of the Thirty Eighth Spring Conference of
the Union of Bulgarian Mathematicians
Borovetz, April 1–5, 2009

DUMPING OF CAPILLARY-GRAVITY WAVES IN A CHANNEL: THE WEDGE DISSIPATION EFFECT*

Dimitar Iliev, Stanimir Iliev

This paper presents first a numerical investigation into a novel class of wave motions in narrow open channels. The distinctive condition on these motions is that: – dissipation in vicinity of contact line is described by De Gennes approach; – the macroscopic lines of contact between the free surface and the sides of the channel move with velocity proportional to cosine of dynamic contact angle; – the effect of the contact angle hysteresis is included; – there are no restriction to the equilibrium contact angle to be close to 90 degrees. We obtain the time evolution of the waves. We investigate influense of the wedge dissipation on the damping rate and frequency of the waves.

There is a large body of literature dealing with the wave motion in an unbounded fluid. A number of analytical, experimental and numerical studies exist on liquid sloshing in containers, mostly in simple rectangular, cylindrical and spherical geometries and for vertical walls. Usually extreme case when the free surface meets the boundary orthogonally is considered in analytical and in numerical studies. This case is known as "free-end edge condition". Benjamin and Scott [1] proposed another extreme boundary condition, known as "stick condition" at the edge of the free surface, namely that contact line between the free surface and sides of the channel is fixed in its equilibrium positions. They argue this condition with phenomenon of contact angle hysteresis. Hocking [2] firstly suggests to apply the universal contact line moving models to obtain the boundary condition for waves in container. He proposed simplest, non-trivial, linear hypothesis for the determination of unsteady contact-line motion when equilibrium contact angle is close to 90°. He postulates that effect of viscosity in the boundary layers on the wall leads to relation (referred as the wetting condition):

$$\frac{\partial \eta}{\partial t} = \lambda \frac{d\eta}{dn} \tag{1}$$

where η is the free surface elevation, t is the time, n is normal to the solid boundary drawn into the fluid and λ is some constant.

*2000 Mathematics Subject Classification: 35J50, 65K10, 76B15.
Key words: Capillary-Gravity waves, contact line dissipation, contact angle hysteresis.
S. Iliev has received financial support from the NSF-Bulgaria under grants number VU-MI-102/05 and INZ01/0117.

Developped Hocking's model is proposed by De Gennes [3]. This approach determines the rate of energy dissipation T in the vicinity of the contact line using molecular-kinetic and hydrodynamic reasons and relates this dissipation to the unbalanced Young force:

$$\partial T/\partial v = \gamma\,(\cos\theta - \cos\theta_{eq}) \tag{2}$$

where θ and θ_{eq} are observed (and therefore macroscopic) dynamic and equilibrium contact angles, γ is liquid/vapour surface tension (in details see [4, 5]). In this work we shall consider simple form of the energy T dissipated in the system per unit time with vicinity of the contact line per unit length of the wetting line is [4–6]:

$$T = \xi\,(\partial\eta/\partial t)^2\big/\,2 \tag{3}$$

where ξ is a friction dissipation coefficient (ξ has the units of viscosity). More general case we shall investigate in other work. Substituting (2) in (1), and denoted by $\lambda = \gamma/\xi$ we obtain

$$\partial\eta\big/\partial t = \lambda\,(\cos\theta - \cos\theta_{eq}) \tag{4}$$

For $\theta_{eq} = 90^\circ$ and for small variation of the dynamic angle $|\theta_{eq} - \theta| \sim 0^\circ$ ($\cos\theta \sim \partial\eta/\partial n$) Equation (3) is identical to Equation (1). In model (3) coefficient λ is well founded and may be obtained in another geometries experimentally [7].

Hysteresis effect can be added in model by substituting in (3) equilibrium angle θ_{eq} with stationary advancing angle θ_a or stationary receding angle θ_r. When angle is in interval $\theta \in [\theta_r, \theta_a]$ contact line is fixed:

$$\frac{\partial\eta}{\partial t} = \lambda\Phi\,(\theta,\theta_r,\theta_a)\,; \quad \Phi\,(\theta,\theta_r,\theta_a) = \begin{cases} 0 & \text{if} \quad \theta \in [\theta_r,\theta_a] \\ \cos\theta - \cos\theta_a & \text{if} \quad \theta > \theta_r \\ \cos\theta - \cos\theta_r & \text{if} \quad \theta < \theta_r \end{cases} \tag{5}$$

Our goal is to test firstly model (4) for capillary-gravity waves. In this work we are interested in the small-amplitude wave motion of the interface, since the outer region viscous dissipation is assumed to be negligible with respect to that in the edge region, nonviscous hydrodynamics needs to be applied.

We consider the 2D motion of an incompressible liquid in a rectangular homogeneous solid channel with vertical walls under the action of the surface tensions γ, γ_v, γ_s (liquid/vapour, vapour/solid and liquid/solid, respectively) and gravity $\mathbf{g}$ force (see Fig. 1). The equilibrium contact angle θ_{eq} satisfy the well-known Young equation $\cos\theta_{eq} = (\gamma_v - \gamma_s)\big/\gamma$. A Cartesian coordinate system (x, y) depicted in Fig. 1 is employed. The distance between the walls L_0, L_a is a; L_{bot} is the channel bottom; depth is a. We denote by S the liquid domain, by $L \equiv \left\{\mathbf{R}^L = \left(R_x^L, \eta\right)\right\}$ – liquid interface with the boundaries $\mathbf{A}_0$ and $\mathbf{A}_a$.

All lengths are normalized by a, time by $\sqrt{a/g}$, velocities by $\sqrt{ag}$, acceleration by g. We are interested in the small-amplitude wave motion of the interface, so we can neglect the fluid viscosity and assume that the energy is dissipated only at the contact line. The liquid flow in $S = \{R\,(x, y)\}$ is assumed to be irrotational, therefore it can be described in terms of the velocity potential φ; $\mathbf{v} = \operatorname{grad}\varphi$. We use dimensionless surface tension $\gamma = \gamma/\rho g a^2$, $\lambda = \lambda\sqrt{ag}$ and the renormalized $\varphi = \varphi/a\sqrt{ag}$. The φ must satisfy the Laplace equation in the domain S:

$$\nabla^2\varphi\,(R,t) = 0, \quad R(x,y) \in \mathrm{S}. \tag{6}$$

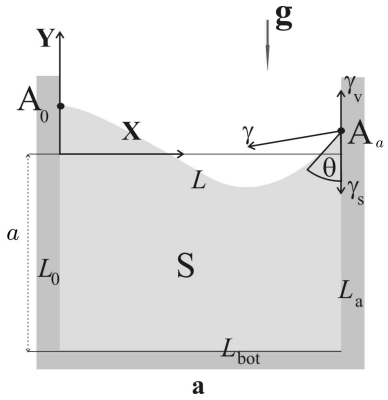

Fig. 1. Definition sketch

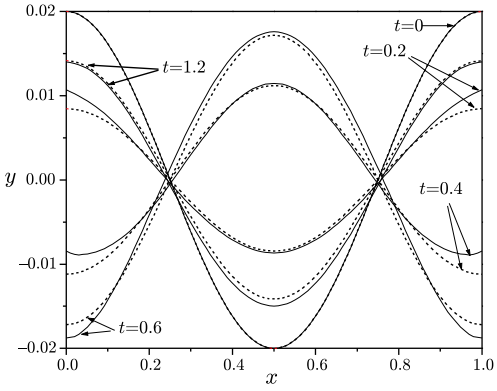

Fig. 2. Solid lines – numerical solution for $\lambda = 4$. Dashed lines – analytical solution from Equation (13) with $\alpha = 0.22$

The container bottom and walls are rigid and impermeable, therefore

$$\partial\varphi\left(R,t\right)/\partial x = 0, \quad R \in \{L_0, L_a\}\,,\ \partial\varphi\left(R,t\right)/\partial y = 0, \quad R \in L_{bot}. \tag{7}$$

the dynamic boundary condition on L is based on the Bernoulli equation and is given by

$$\partial\varphi\left(\mathbf{R}^L,t\right)/\partial t = -v^2\left(\mathbf{R}^L,t\right)/2 - R_y^L + \gamma L_{xx}\Big/\left(1+L_x^2\right)^{3/2};\ \mathbf{R}^L \in L/\{\mathbf{A}_0 \cup \mathbf{A}_a\}, \tag{8}$$

in inner point of L and in boundary points

$$\partial\mathbf{A}_0/\partial t = \lambda\Phi\left(\theta,\theta_r,\theta_a\right);\partial\mathbf{A}_a/\partial t = \lambda\Phi\left(\theta,\theta_r,\theta_a\right). \tag{9}$$

We solve (6)–(9) using the numerical method, described in [8]. But two modifications are made. First, when update the harmonic potential at the free line using equations (8), we add capillary term. And second – Equation (9) is used for boundary condition of Laplace equation. To do this we take into account the relations:

$$F_{2,101} - F_{2,100} = \Delta_2\lambda\Phi\left(\theta\left(\mathbf{A}_0\right)\right);\ F_{100,101} - F_{100,100} = \Delta_{100}\lambda\Phi\left(\theta\left(\mathbf{A}_a\right)\right)$$

when we obtain the minimum of the function of variables $F_{i,j}$, $i = 2, 100; j = 2, 100$.

For the case $\theta_a = \theta_r = 90°$, free-end edge condition (dynamic contact angle is fixed at 90°), and for initial shape of interface

$$\eta\left(x,0\right) = \varepsilon\cos 2\pi x \tag{10}$$

where ε is a small parameter, the motion is standing wave [9]:

$$\eta\left(x,t\right) = \varepsilon\cos\omega t\cos 2\pi x \tag{11}$$

where

$$\omega = \sqrt{2\pi\left(1+4\gamma\pi^2\right)\tanh 2\pi}. \tag{12}$$

In our model this case corresponds to $\xi = 0$ (no dissipation). We analyse how the dissipation affects the wave motions, comparing our results with equation

$$\eta\left(x,t\right) = \varepsilon\ \cos\omega t\ \cos 2\pi x\ \exp(-\alpha t) \tag{13}$$

which is modification of the solution (11) with added damping term with coefficient α.

Numerical results. In this work we consider case γ =0.1 because for this value of

γ influence of gravity and capillary into frequency are of one order (see Equation (12)). As initial position of the free surface and the initial distribution of the potential we take here $\eta(x,0) = 0.02\cos 2\pi x$ and $\varphi(R,0) = 0$.

First we shall consider the case $\theta_a = \theta_r = 90°$. Our results in this case can be compared with Hocking results (model Equation (1)) since in this case difference between right parts of Equation (1) and Equation (4) is very small (for $|\theta - 90°| < 10°$, $|\cos\theta - \operatorname{cotg}\theta| < 0.0026$).

Free lines from our numerical results are shown in Fig. 2 for $\lambda = 4$ (with solid lines), and from analytical solution from Equation (13) for α=0.22 (with dashed lines). Both solutions are shown in moments of time $t = 0$; 0.2; 0.4; 0.6; 0.8; 1; 1.2 (the period in this case is approximately 1.13). Function (13) describes well the central part of numerically obtained dumping waves. But that function can't describe well the behavior of contact line around borders.

Our results show that the relation between dissipation coefficient ξ and damping coefficient α is complicated. For waves with small amplitude, when $\xi \sim 0$, dissipation per period is small and increases when ξ increases. But when $\xi/\gamma \gg 1$ contact line motion is very slow and dissipation per period is very small again. This behavior is similar to the dependence $\alpha(\lambda)$ in Hocking's model (Equation (1)) given in table 1 and figure 1 in Ref [2]. In Fig. 3 is shown the time evolution of the border point (with initial height 0.02) and middle point (with x-coordinate 0.5 and initial height -0.02) for different values of λ. In Fig. 3(a) $\lambda = 6$; 4; 2; 1; 0.7 and in Fig. 3(b) $\lambda = 0.3$; 0.2; 0.08; 0.05; 0.02. As one can see in Fig. 3a, border and middle points of the contact line oscillate around equilibrium zero position of the free line. Also dumping for one period increases when λ decreases. But for small values of λ, when λ decreases damping of middle point increases. Also on Fig. 3 is seen another model characteristic, predicted in Ref. [2] - frequency of oscillations decreases when λ increases. For λ=2 the period is approximately 1.12 and for $\lambda = 0.02$ the period is approximately 0.8.

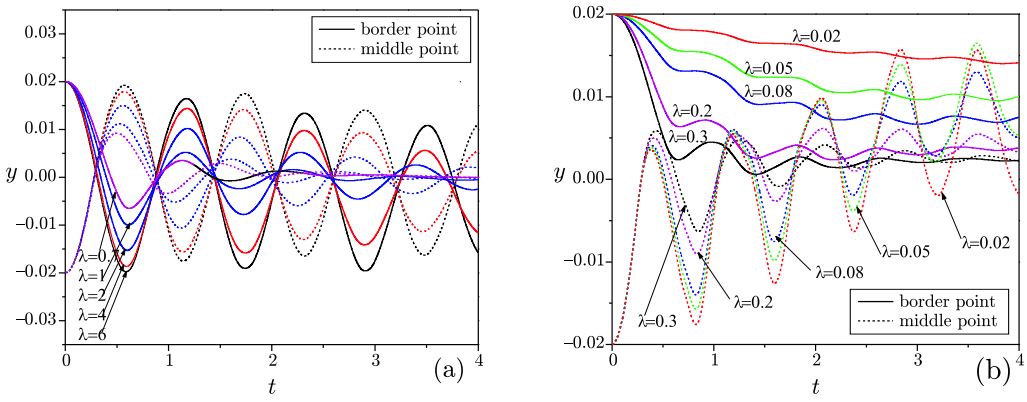

Fig. 3 The time evolution of the border point – solid lines and the middle point – dashed lines for (a) $\lambda = 6$; 4; 2; 1; 0.7; (b) $\lambda = 0.3$; 0.2; 0.08; 0.05; 0.02.

Now we shall consider the wave evolution for $\theta_a = \theta_r \neq 90°$ and for $\theta_a \neq \theta_r$. Hocking's model doesn't describe these. In Fig. 4 is shown time evolution of the left border point

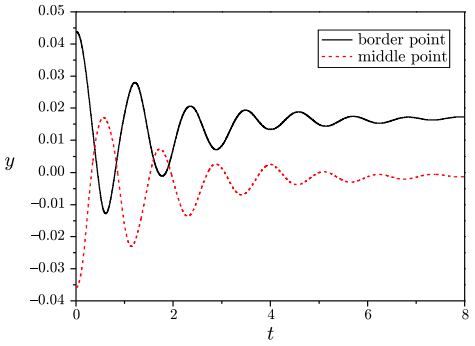

Fig. 4. The time evolution of the border point – solid line and the middle point – dashed line for $\lambda = 2$, $\theta_{eq} = 85°$

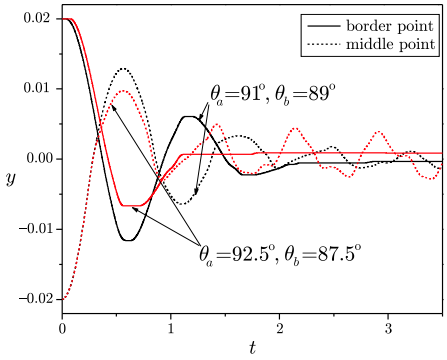

Fig. 5. The time evolution of the border point – solid line and the middle point – dashed line for $\lambda = 2$, $\theta_a = 92.5°$, $\theta_r = 87.5°$ and for $\lambda = 2$, $\theta_a = 91°$, $\theta_r = 89°$

and middle point for $\theta_a = \theta_r = 85°$, λ=2. In this case these points converge to different high positions.

Evolution of the wave when hysteresis is included in model (4) is shown in Fig. 5 for two different values of hysteresis: $\theta_a - \theta_r = 2°$ and $\theta_a - \theta_r = 5°$. The evolution of the left border point and middle point of wave is shown in Fig. 5 for λ=2 when $\theta_a = 91°, \theta_r = 89°$ – with solid lines and when $\theta_a = 92.5°, \theta_r = 87.5°$ – with dashed lines respectively. In this case the border points realize the stick-slip motion.

In "stick regime" there is no dissipation in the waves.

REFERENCES

[1] T. B. Benjamin, J. C. Scott. Gravity-capillary waves with edge constraints. *J. Fluid Mech.*, **92** (1979), 241–267.

[2] L. M. Hocking. The damping of capillary-gravity waves at a rigid boundary. *J. Fluid Mech.*, **179** (1987), 253–266.

[3] P. G. De Gennes. Wetting: statics and dynamics. *Rev. Mod. Phys.*, **57** (1985), 827–863.

[4] M. J. de Ruijter, J. de Coninck, G. Oshanin. Droplet Spreading: Partial Wetting Regime Revisited. *Langmuir*, **15** (1999), 2209–2216.

[5] S. Iliev, N. Pesheva, V. S. Nikolayev. Quasistatic relaxation of arbitrarily shaped sessile drops. *Phys. Rev. E*, **72** (2005), 011606.

[6] T. D. Blake. The physics of moving wetting lines. *J. Colloid Interface Sci.*, **299** (2006), 1–13.

[7] S. Iliev, N. Pesheva, V. S. Nikolayev. Dynamic modelling of contact line deformation: comparison with experiment. *Phys. Rev. E*, **78** (2008), 021605.

[8] D. Iliev. Local variation method to calculate two dimensional gravity waves in container. *Math. and Education in Math.*, **36** (2007), 240–245.

[9] W. G. Penney, A. T. Price. Some gravity wave problems in the motion of perfect liquids. Part II. Finite periodic stationary gravity waves in a perfect liquid. *Philos. Trans. R. Soc. London*, Ser. A **244** (1952), 254–284.

Dimitar Iliev
Department of Mathematics and Informatics
Sofia University
5, J. Bourchier Str.
1164 Sofia, Bulgaria
e-mail: diliev@fmi.uni-sofia.bg

Stanimir Iliev
Institute of Mechanics
Bulgarian Academy of Sciences
G. Bonchev Str., Bl. 4
1113 Sofia, Bulgaria
e-mail: stani@imbm.bas.bg

ЗАТИХВАНЕ НА КАПИЛЯРНО-ГРАВИТАЦИОННИ ВЪЛНИ В КАНАЛ: ЕФЕКТИ НА ДИСИПАЦИЯТА ОТ ОБЛАСТТА НА ТРИФАЗЕН КОНТАКТ

Димитър Илиев, Станимир Илиев

В статията е представено числено изследване на нов клас вълнови движения, имащи място в тесни отворени канали. Отличителните условия на тези движения са: – дисипацията на енергия от околността на контактната линия се описва чрез подхода на Де Жан; – микроскопическата трифазна контактна линия се движи със скорост, която е пропорционална на косинуса на динамичния контактен ъгъл; – включен е ефекта на хистерезис на контактния ъгъл; няма ограничения равновесния контактен ъгъл да е 90 градуса. Ние сме намерили времевото изменение на формата на вълните. Зависимостта на скоростта на затихване и на честотата на вълните от величината на дисипация от областта на трифазен контакт е изследвана.